Progress In Electromagnetics Research C, Vol. 82, 13–27, 2018

A Very Compact MIMO Antenna with Triple Band-Notch Function for Portable UWB Systems

Chandrasekhar R. Jetti[1, *] and Venkateswara R. Nandanavanam[2]

Abstract—A very compact triple band-notched multiple input multiple output antenna (MIMO) for ultra-wideband (UWB) communications is fabricated on an FR4 dielectric substrate having the overall size of $18 \times 21 \times 0.8\,\text{mm}^3$. The proposed antenna consists of two rectangular metal monopoles which are excited by 50-Ω microstrip lines on top of a substrate, and a common protrude ground is at the bottom. To achieve low mutual coupling between radiating elements, a T-shaped stub is protruded from the ground plane. By etching two C-shaped slots on the radiating patches, band-notched functions at 5.15–6 GHz and 7.8–8.4 GHz are obtained. The third notch band from 3.3–3.7 GHz is realized by adding U-shaped metal strips to the ground. The measured and simulated results demonstrate that the proposed antenna offers good impedance bandwidth of $|S_{11}| \leq -10\,\text{dB}$ from 2.8–12.2 GHz covering whole UWB band except at the designed notch bands, while giving less mutual coupling ($|S_{21}|$) of lower than $-25\,\text{dB}$ in the whole UWB band. The measured envelope correlation coefficient (ECC < 0.013), nearly constant gain and stable radiation patterns show that the proposed MIMO antenna is an appropriate candidate for portable UWB systems.

1. INTRODUCTION

Higher data rates and improved quality of service are the primary concerns of future wireless communication systems like 4G and 5G. Since Federal Communications Commission allocated the unlicensed frequency spectrum from 3.1–10.6 GHz for commercial applications in 2002 [1], ultra-wideband (UWB) technology has attained considerable attention because of its inherent features such as high data rate communications, extremely low power consumption, and low cost. However, for UWB communication systems, frequency interference and multipath fading are two significant issues which should be solved.

Ultra-wideband is a trending technology for short range low power communications. It makes use of short duration pulses which have very low power spectral density for transmission of data. So, UWB system could easily interfere with existing narrowband communication systems such as WiMax (Worldwide Interoperability for Microwave Access-3.3–3.7 GHz), WLAN (Wireless Local Area Network-5.15–5.825 GHz), and X-band satellite communication (7.9–8.4 GHz). Therefore, a notch at the interfering frequency is needed to combat its effect. Designing UWB antenna with integrated frequency notching function is a good solution to suppress the frequency interference and reduces the complexity of the UWB system instead of using a conventional filter.

The primary uses of UWB technology are for WPANs (wireless personal area networks) and WBANs (wireless body area networks) in an indoor ambiance where the rich multipath propagation leads to inter-symbol interference (ISI). Hence, communication range and quality of service are significantly

Received 12 January 2018, Accepted 26 February 2018, Scheduled 9 March 2018

* Corresponding author: Chandrasekhar Rao Jetti (jettychandu@gmail.com).

[1] Department of ECE, University College of Engineering and Technology, Acharya Nagarjuna University, Guntur and Koneru Lakshmaiah Education Foundation, Vaddeswaram, Guntur, Andhra Pradesh, India. [2] Department of ECE, Bapatla Engineering College, Bapatla, Andhra Pradesh, India.

reduced. In recent times, multiple input multiple output (MIMO) technology has attained much attention in wireless communication applications because it exploits multipath to increases the range of communication and link quality without consuming additional frequency spectrum and signal power. Thus, multiple antennas or MIMO technology is a promising solution for multipath fading problem in UWB system [2, 3].

However, MIMO system performs well when the signals are highly uncorrelated on different antennas. So, accommodating multiple antennas with low correlation and hence less mutual coupling (or high isolation between ports) between them in space-limited portable devices is always a challenging task for antenna designers [4]. Hence, from the above reasons, designing compact UWB MIMO antennas providing band-notch characteristics and low mutual coupling is imperative.

Various designs have been proposed in the recent years to suppress the effects of mutual coupling in UWB MIMO antennas [5–10], which are composed of using tree-like structure on the ground [5], placing radiators perpendicular to each other and adding two long protruding stubs to ground [6], adopting wideband neutralization line [7], introducing a T-shaped slot and line slot on the ground [8], using a modified ground structure along with a T-shaped slot on the ground [9], or adopting a Y-shaped slot on the T-shaped protruded ground [10]. However, the antenna designs in [5–10] do not offer band-notch properties.

A number of experiments were done earlier to integrate the single and multiple band-notch functions for UWB systems and hence to mitigate the frequency interference from narrowband systems [11–26]. Methods such as etching $\lambda/4$ and $\lambda/2$ resonators on the ground [11], introducing split-ring resonator (SRR) slots on radiator [12], incorporating two rectangular strips on the ground plane [13], etching a 1λ slot into radiator [14], slitting $\lambda/4$ open-ended L-shaped slots on the radiator elements [15], employing $\lambda/4$ and $\lambda/2$ resonators [16], and using elliptical SRR on the radiator [17]. The proposed antennas in [11–17] mostly reject WLAN band only. Dual band-notched functions for UWB-MIMO antennas can be realized by employing nested C-shaped slots in the patch [18], etching 1λ loop path and 0.25λ slot on radiator [19], introducing strips beneath the patch [20], placing open-ended slot and SRR in the ground [21], placing a parasitic strip and open-ended slot on ground [22], or by loading trident-shape strip on the patch [23].

Recently, some papers have been presented to achieve triple band-notched functions for UWB MIMO systems [24–26]. A compact UWB antenna having $30 \times 60\,\text{mm}^2$ with triple notches for polarization diversity applications was designed in [24]. Two complementary SRRs and a C-shaped strip were employed to get rejected bands at WiMax/WALN and X-bands, respectively. A miniaturized MIMO antenna of dimensions $28 \times 22\,\text{mm}^2$ for UWB applications was developed in [25]. Triple band-notched properties at WiMax/WLAN/X-bands can be realized by adding two C-shaped slots into the radiator. In [26], a compact CPW-fed isolation-enhanced MIMO antenna of size 26.75 mm × 41.5 mm with Minkowski fractal DGS for UWB applications was developed. Identical rectangular slots on a ground plane and rotated C-shaped slots from radiator were used to achieve triple rejected bands at 3.3–3.7, 3.7–4.2, and 5.15–5.85 GHz, respectively. The antennas reported in [24–26] have three notched bands with good isolation, but they are not compact enough, and antenna designs are somewhat complex. So, there is a need for the design of simple, isolation-enhanced and very compact band-notched UWB MIMO antennas for portable devices.

In this paper, a very compact MIMO antenna with three notched bands for portable UWB systems is proposed. Overall size of the antenna is $18 \times 21 \times 0.8\,\text{mm}^3$ which is very small compared to the antennas reported in [24–28]. Two simple planar monopole elements are used as antenna elements of the UWB MIMO antenna, fed by a 50-Ω microstrip line. A T-shaped stub is introduced on the ground plane to achieve good antenna matching and very low mutual coupling between the radiating elements. The proposed antenna provides good impedance bandwidth ($S_{11} \leq -10\,\text{dB}$) from 2.8–12.2 GHz and mutual coupling (S_{21}) of less than −25 dB. Two split rectangle ring slots (C-shaped slots) namely Slot-1 and Slot-2 are etched on the radiating elements to mitigate the interference from 5.15–6 GHz and 7.8–8.4 GHz, respectively. The notches in the proposed antenna are not exclusive to each other like the notches in [28]. In addition, a U-shaped strip is added to the ground plane to reject the frequency interference from 3.3–3.7 GHz. The detailed description of the proposed antenna is given in further sections.

2. ANTENNA DESIGN

2.1. Geometry

The optimized geometry of the proposed triple band-notched UWB MIMO antenna and a photograph of the fabricated antenna are shown in Figs. 1(a) and 1(b). The antenna is fabricated on a low-cost FR4 PCB substrate with relative permittivity (ε_r) of 4.4, loss-tangent of 0.02 and substrate thickness of 0.8 mm. The overall size of an antenna is $18 \times 21 \times 0.8\,\text{mm}^3$ which is very small compared to the antennas mentioned in [24–28]. The proposed antenna comprises two radiating elements which are horizontally placed on top of the substrate to save space. Each radiating element is fed by a 50-ohm microstrip line. A $L_G \times W$ size ground part and a T-shaped ground part constitute a ground plane which is printed on the bottom side of the substrate. The T-shaped ground stub consists of a vertical strip ($S_{L1} \times S_{W1}$) and horizontal strip ($S_{L2} \times S_{W2}$). A T-shaped stub is extended from the common ground plane to improve the antenna impedance matching and suppress the mutual coupling. The T-shaped stub on the ground plane performs two major functions: extending the current path, which can lower the first cutoff frequency of the monopole antenna, and suppressing the surface currents to weakens the mutual coupling in UWB range. A pair of C-shaped slots denoted as Slot-1 and Slot-2 were introduced on the radiating elements to perform band-notching functions from 5.15 to 6 GHz (WLAN) and 7.8 to 8.4 GHz (X-band satellite communication), respectively. To create a third notched band from 3.3 to 3.7 GHz (WiMax), a pair of U-shaped strips are joined to the ground plane.

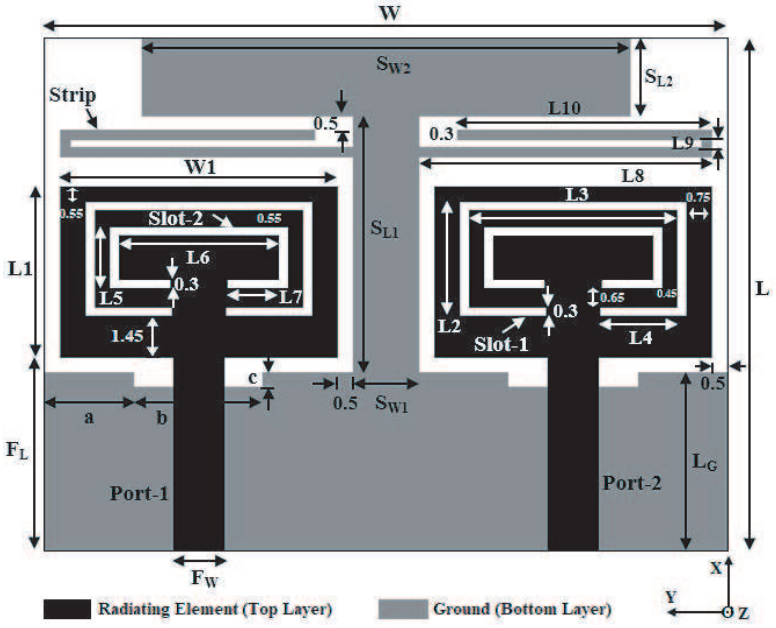

(a)

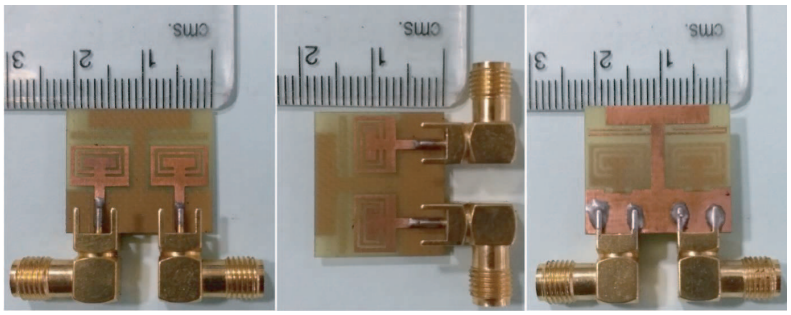

(b)

Figure 1. (a) optimized geometry of the proposed antenna, and (b) fabricated antenna.

The proposed antenna design, dimensions optimization, and simulations are carried out using Ansoft HFSS v.13 (High Frequency Structure Simulation). The optimized dimensions of the proposed antenna are given as follows: (unit: mm): $L = 18$, $W = 21$, $L1 = 6$, $W1 = 8.5$, $F_L = 6.8$, $F_W = 1.53$, $L2 = 4$, $L3 = 6.4$, $L4 = 2.4$, $L5 = 2.2$, $L6 = 4.9$, $L7 = 1.6$, $L8 = 9$, $L9 = 0.3$, $L10 = 7.8$, $L_G = 6.25$, $a = 2.75$, $b = 4$, $c = 0.5$, $S_{L1} = 9$, $S_{W1} = 2$, $S_{L2} = 2.75$, and $S_{W2} = 15$. The proposed antenna is fabricated with the above parameters and is displayed in Fig. 1(b).

2.2. Design Process and Working Mechanism

Evolution of the compact triple band-notched UWB MIMO antenna is presented in Figs. 2(a)–(e). The subsequent sections describe design process of the proposed antenna, effect of a T-shaped stub, and effects of Slot-1, Slot-2 and strips.

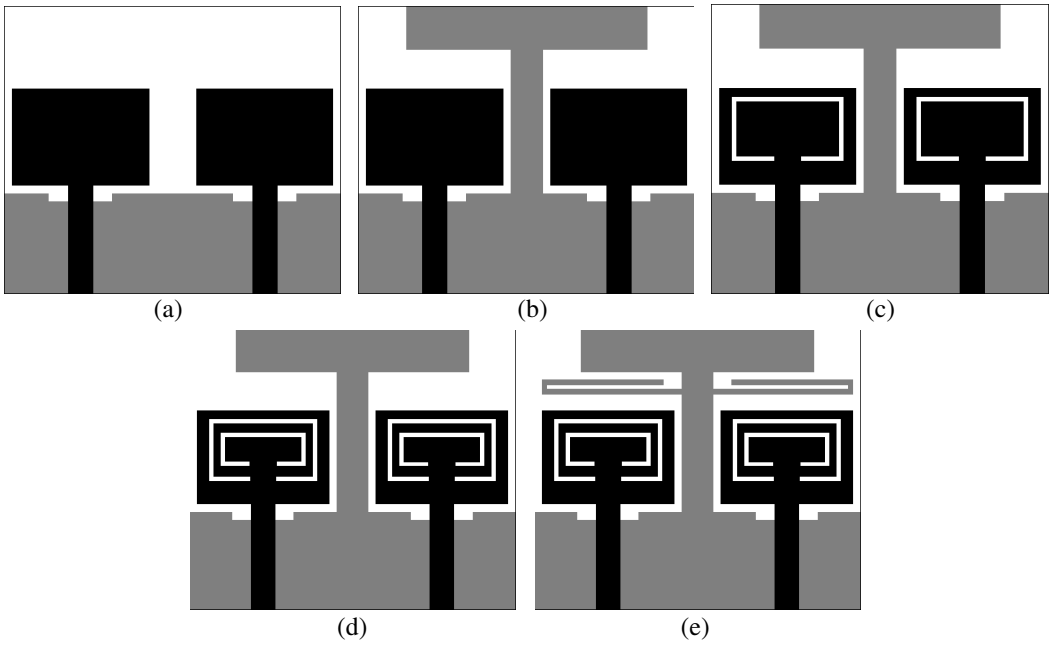

Figure 2. Evolution of the proposed antenna: (a) UWB MIMO antenna without T-shaped stub, (b) UWB MIMO antenna with T-shaped stub (Antenna-1), (c) UWB MIMO antenna with band-notch at WLAN (Antenna-2), (d) UWB MIMO antenna with band-notches at WLAN and X-band (Antenna-3), and (e) proposed antenna.

2.2.1. UWB-MIMO Antenna

A rectangular monopole antenna element of size $L1 \times W1$ which is excited by a microstrip line (port) forms an element for the UWB MIMO antenna as shown in Fig. 2(a). The microstrip line width F_W is chosen as 1.53 mm to get characteristic impedance of 50-ohms.

2.2.2. Effect of T-Shaped Stub on MIMO Antenna

Since the sizes of radiating monopoles and ground plane are very small, surface currents on the ground and near-field radiation cause poor impedance matching and strong mutual coupling between the MIMO antenna elements, which limits the system performance. Fig. 3 clearly shows that the UWB MIMO antenna without T-shaped ground stub has a low resonant frequency of about 4.4 GHz ($|S_{11}| < -10$ dB) which is higher than 3.1 GHz needed for UWB system, and mutual coupling ($|S_{21}|$) of about -10 dB is observed between the two ports as shown in Fig. 4(a). However, UWB MIMO antenna with a T-shaped ground stub (indicated as Antenna. 1) creates resonance at about 4 GHz with low cutoff frequency at

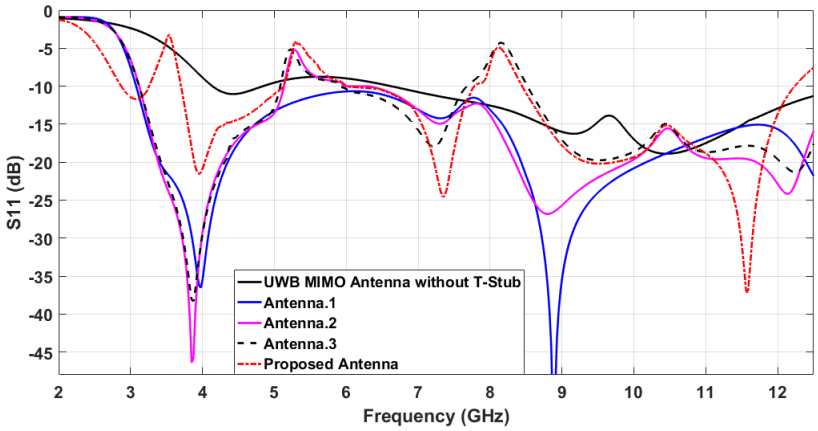

Figure 3. Comparison of S_{11}-parameter at various stages of proposed antenna.

about 3 GHz. It can be observed from Fig. 3 and Fig. 4(a) that UWB MIMO antenna with a T-shaped ground stub covers the entire UWB range from 3.1 to 10.6 GHz with a good impedance bandwidth of $|S_{11}| \leq -10$ dB and mutual coupling of lower than -25 dB, respectively. Hence, the T-shaped ground stub is used to improve impedance matching for the antenna and to weaken the mutual coupling by reflecting the radiation from the radiating monopoles. The S-parameters (S_{11} and S_{21}) of an antenna for different lengths (S_{W2}) and widths (S_{L2}) of the horizontal strip of T-stub are plotted in Figs. 4(b) and 4(c). It is evident from Figs. 4(b) and 4(c) that the total length and width of the T-stub has more impact on impedance matching than the mutual coupling. Because of symmetrical structure of the proposed antenna, S_{11} is the same as S_{22}, and S_{21} is the same as S_{12}. Therefore, only S_{11} and S_{21} are plotted in Figs. 4(b) and 4(c). Moreover, Fig. 4(d) illustrates the surface current distribution at 7 GHz without and with a T-shaped stub when port-1 is excited. As seen from Fig. 4(d), a huge amount of current flows from port-1 to port-2 through the common ground when no stub in between antenna elements. On the other hand, with a T-stub, the orientation of surface currents is diverted, because it can act as a reflector, and also the distance between the ports is increased. Hence, most of the current is blocked by the stub, and very little current enters into port-2 from port-1. Therefore, the T-shaped stub improves isolation in the proposed MIMO antenna system.

2.2.3. Effect of Slot-1, Slot-2, and Strips on S_{11}

The band-notch characteristics for UWB systems can be obtained by etching slots or SRRs on the radiating element or ground plane or feed line. This can also be done by adding strips or stubs adjacent to the radiator or ground or feed line as discussed in [11–28]. Each slot or strip can function as a resonator, and the slot or strip length controls the notch center frequency. However, the desired notch band is obtained by proper tuning of length and width of the slot or strip. The width of the slot or strip has a negligible effect on the notch-band position, but it has a significant effect on notch bandwidth. The total lengths of etched slots or added strips should be $\lambda/2$ or $\lambda/4$ corresponding to the notched-band center frequency, where λ is the guided wavelength ($\lambda = \frac{c}{f_{notch}\sqrt{\varepsilon_{eff}}}$) as given in Equations (1) and (2) [11].

$$L_{Notch} = \frac{c}{2f_{Notch}\sqrt{\varepsilon_{eff}}}, \tag{1}$$

$$L_{Notch} = \frac{c}{4f_{Notch}\sqrt{\varepsilon_{eff}}}, \tag{2}$$

where c denotes the light speed, f_{Notch} the notch center frequency, L_{Notch} the total length of slot or strip, and $\varepsilon_{eff} = (1 + \varepsilon_r)/2$ the effective dielectric constant.

To create a first band-notch function at 5.15–5.85 GHz WLAN band, Slot-1 is introduced on each element of Antenna-1 which forms Antenna-2 as displayed in Fig. 2(c). The total length of Slot-1 is

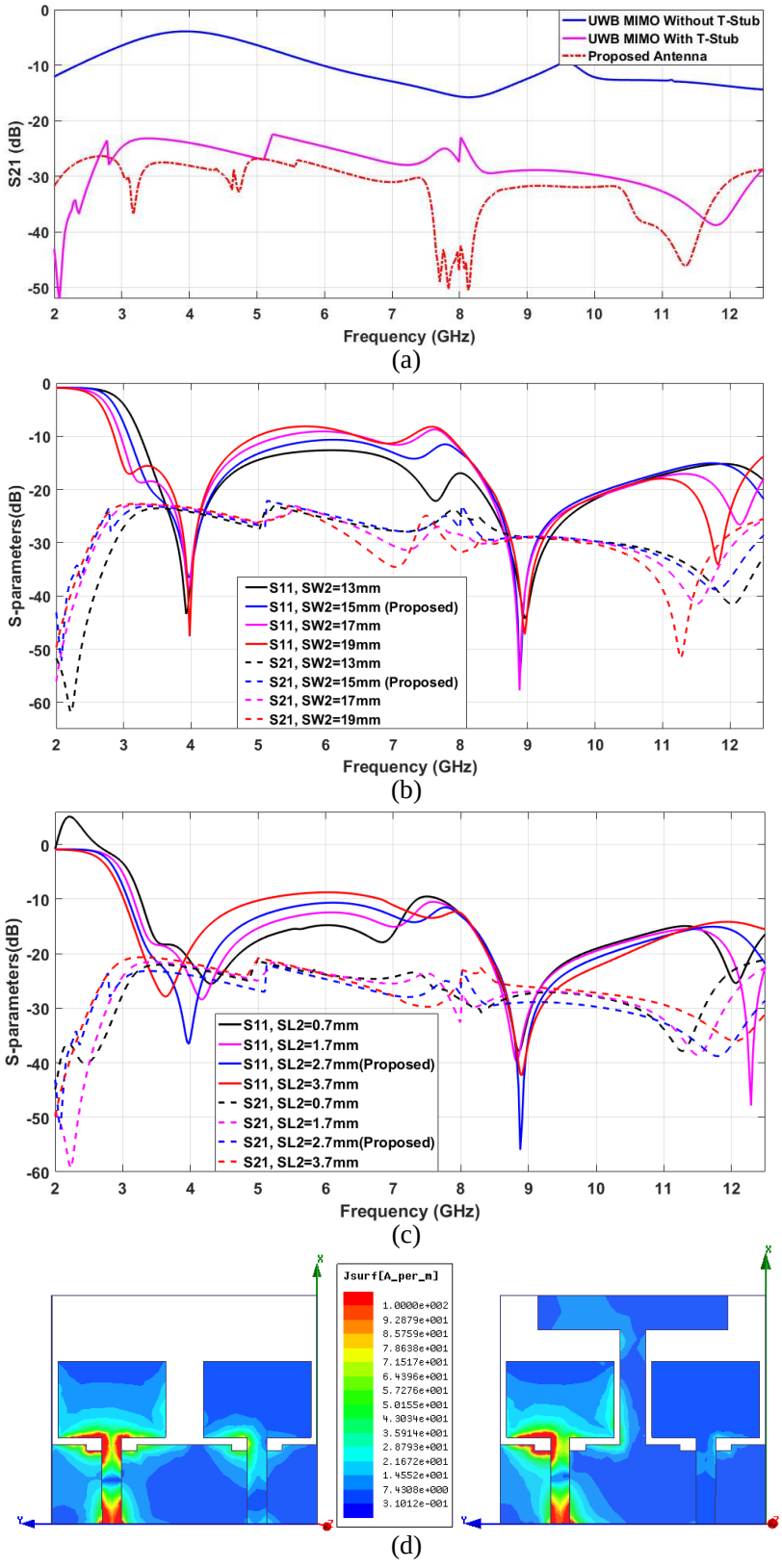

Figure 4. (a) Comparison of S_{21}-parameters, (b) S-parameters for different lengths of T-stub, (c) S-parameters for different widths of T-stub and (d) current distribution on MIMO antenna.

deduced approximately by using Equation (3).

$$L_{Slot-1}(at\ 5.5\,\text{GHz}) = 2(L2 + L4) + L3 \approx \frac{\lambda}{2}. \tag{3}$$

The calculated total length of Slot-1 using Equation (1), when $f_{Notch} = 5.5\,\text{GHz}$ and $\varepsilon_r = 4.4$, is 16.59 mm whereas the designed length based on Equation (3) is 19.2 mm which is approximately equal to half-wavelength at 5.5 GHz. As observed from Fig. 3, Antenna-2 gives band-notching function from 5.15–6 GHz with S_{11} of about -5 dB with the low mutual coupling of less than -25 dB. The effect of Slot-1 on the S_{11} parameter of an antenna is better understood by performing parametric analysis on the length (L4) and width of Slot-1. Fig. 5(a) illustrates the effect of length L4 of Slot-1 on S_{11}-parameter. It is observed that increasing L4 length from 1.2 mm to 2.8 mm, the notch center frequency is reduced from (5.5–6.8 GHz) band to (4.96–5.3 GHz) band. The desired band-notch at 5.15–6 GHz is obtained for $L4 = 2.4$ mm which is adopted in the proposed design. The effect of Slot-1 width on S_{11} for $L4 = 2.4$ mm is depicted in Fig. 5(b). It can be seen that as the width increases from 0.3 mm to 0.36 mm, the lower edge of the notched band remains at 5.15 GHz, but the upper edge shifts up from 6 to 6.7 GHz, increasing the bandwidth of notched band. Thus, the Slot-1 width of 0.3 mm is chosen in the proposed design.

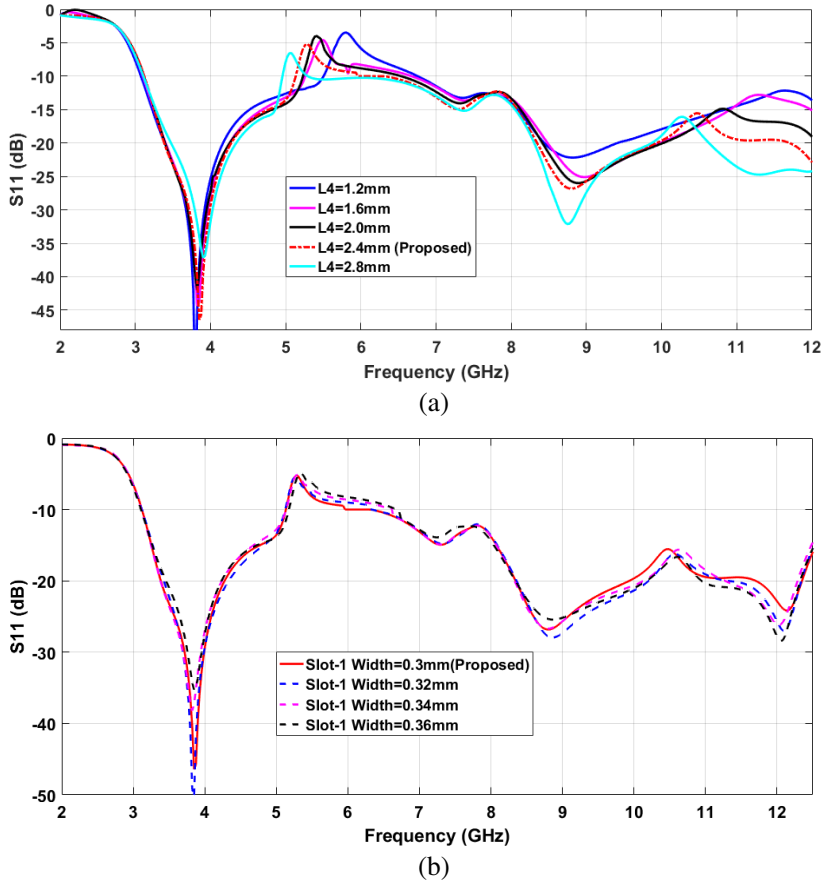

Figure 5. Simulated S_{11} plot for: (a) different values of L4, (b) different Slot-1 widths.

Similarly, another split rectangle ring slot denoted by Slot-2 is etched on Antenna-2 elements to produce Antenna-3 as indicated in Fig. 2(d). As a result, the second notch at 7.8–8.4 GHz X-band uplink satellite communication service in addition to the WLAN band is obtained. The total length of Slot-2 at 8.1 GHz notch frequency is determined using Equation (4) and is around half-wavelength. The simulated length of Slot-2 (12.5 mm) is almost equal to the calculated length (11.27 mm).

$$L_{Slot-2}(at\ 8.1\,\text{GHz}) = 2(L5 + L7) + L6 \approx \frac{\lambda}{2}. \tag{4}$$

Fig. 3 shows $|S_{11}|$ of -5 dB and -4.8 dB from (5.1–5.9 GHz) band and (7.7–8.5 GHz) band, respectively. The effect of Slot-2 on S_{11}-parameter is plotted in Fig. 6(a) for various values of length $L7$. From Fig. 6(a), as length $L7$ rises from 1 mm to 1.8 mm, the first notch band remains unchanged, but the second notch frequency band falls from (8.4–9.1 GHz) to (7.5–8 GHz). In the proposed antenna, $L7 = 1.6$ mm is used to achieve notched-band from 7.9 to 8.4 GHz. The effect of Slot-2 width on S_{11} is depicted in Fig. 6(b) for length $L7 = 1.6$ mm. It can be found that as the width rises from 0.3 mm to 0.36 mm, the upper edge shifts up from 7.9 to 8.6 GHz, increasing the notched bandwidth, while lower edge of the notched band remains at 7.9 GHz. Hence, the Slot-2 width of 0.3 mm is used in the proposed design.

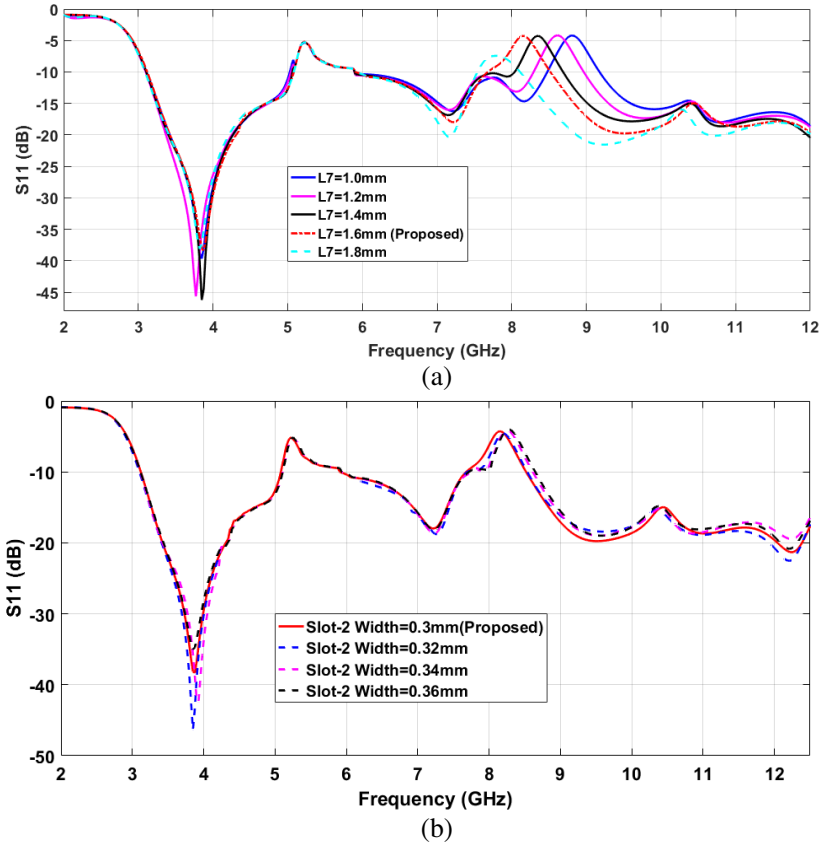

Figure 6. Simulated S_{11} plot for: (a) different values of $L7$, (b) different Slot-2 widths.

Finally, the proposed antenna is formed by joining a couple of U-shaped strips to Antenna-3, shown in Fig. 2(e). Hence, the third band-notch at 3.3–3.7 GHz WiMax band is achieved with inclusion of WLAN and X-band notches. From Fig. 3, it can be easily seen that the proposed antenna is able to reject potential interference from 5.15–6 GHz, 7.8–8.4 GHz, and 3.3–3.7 GHz bands. The total strip length is obtained using Equation (5) and is comparable with a quarter-wavelength at 3.5 GHz.

$$L_{Strip}(at\ 3.5\,\text{GHz}) = L8 + L9 + L10 \approx \frac{\lambda}{4}. \tag{5}$$

The simulated strip length is 17.1 mm, and the calculated length is 13.04 mm. Fig. 3 shows $|S_{11}|$ of -4.1 dB at (5.1–5.9 GHz), -4.89 dB at (7.8–8.4 GHz), and -3.2 dB at (3.3–3.7 GHz) band, respectively. Fig. 7(a) illustrates the strip effects with different L10 values on S_{11}. It can be seen that the third notch band shifts from (3.35–3.87 GHz) to (3–3.5 GHz) as $L10$ changes from 6.8 mm to 8.8 mm keeping other two notch bands unchanged. The strip length $L10$ of 7.8 mm is selected in the design to realize notched-band at 3.3–3.7 GHz. Fig. 7(b) displays the S_{11} parameter for different strip widths keeping $L10$ as 7.8 mm. It can be observed that as the width increases from 0.3 mm to 0.36 mm, the upper

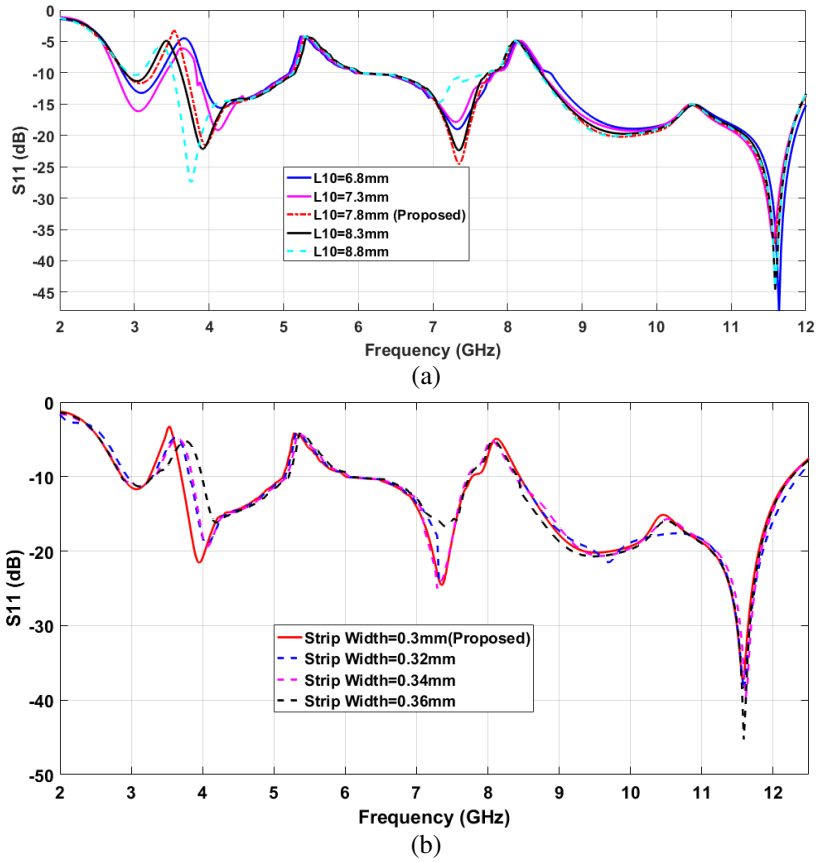

Figure 7. Simulated S_{11} plot for: (a) different values of $L10$, (b) different Strip widths.

edge shifts up from 3.3 to 3.7 GHz, increasing the notched bandwidth, while the lower edge of notched band remains at 3.3 GHz. Therefore, the strip width of 0.3 mm is adopted in the proposed design. Finally, from Figs. 5–7, it is observed that the desired band notch at WLAN/X-band/WiMax band is obtained only when the total length of the resonator (Slot-1/Slot-2/Strip) is equal to the designed length (19.2 mm/12.5 mm/17.1 mm) rather than the calculated length (16.59 mm/11.25 mm/13.04 mm). Thus, a small difference is found between designed lengths and calculated lengths.

To further understand the creation of notched bands, surface current distributions on the proposed antenna at 3.5, 5.2, 8.2, 9.5 GHz are presented in Fig. 8. As described in Fig. 8(a), at 3.5 GHz, since strong current is concentrated on a U-shaped strip, current flow on the antenna is blocked, and hence antenna cannot radiate energy. Thus, band-notch at 3.3–3.7 GHz WiMax band is obtained. As seen from Fig. 8(b), large current is accumulated around Slot-1, which leads to the creation of 5.15–6 GHz WLAN notched band. It is evident from Fig. 8(c) that heavy current is concentrated near Slot-2 at 8.2 GHz which generates the third notched band at 7.8–8.4 GHz X-band uplink satellite communication service. The notches have very large S_{11} values of -3.2, -4.1, and -4.8 dB at 3.5, 5.28, and 8.12 GHz, respectively. At 9.5 GHz, the proposed antenna radiates very efficiently with good impedance bandwidth $|S_{11}| < -10$ dB as shown in Fig. 8(d).

3. RESULTS AND DISCUSSION

3.1. S-Parameters

The measurements of S-parameters of the proposed UWB-MIMO antenna are carried out using Anritsu MS2037C vector network analyzer and an anechoic chamber. Fig. 9 depicts the simulated and measured S-parameters. It is evident from the results that the proposed antenna provides $|S_{11}| < -10$ dB over

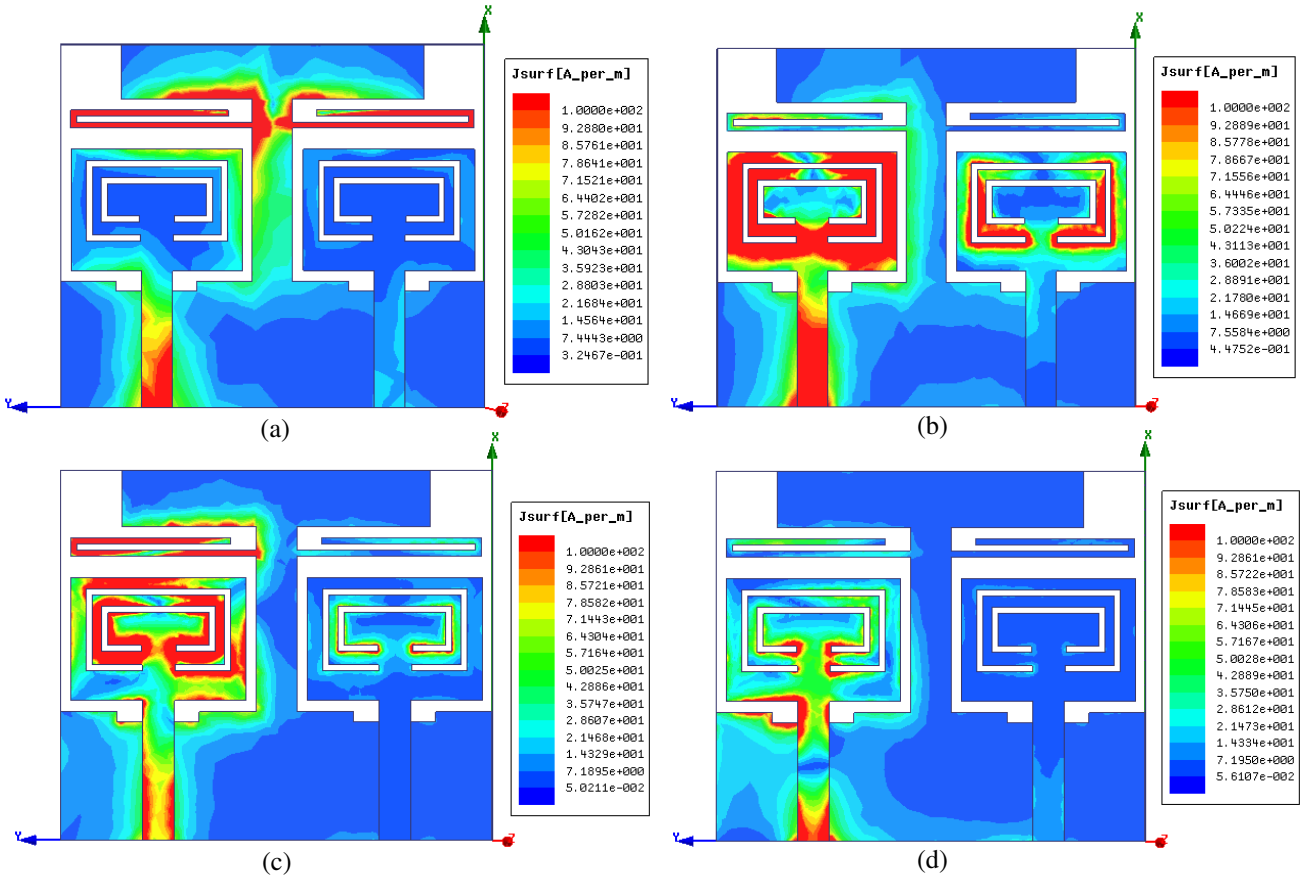

Figure 8. Simulated current distribution on the antenna when port 1 excited at (a) 3.5 GHz, (b) 5.2 GHz, (c) 8.2 GHz, and (d) 9.5 GHz.

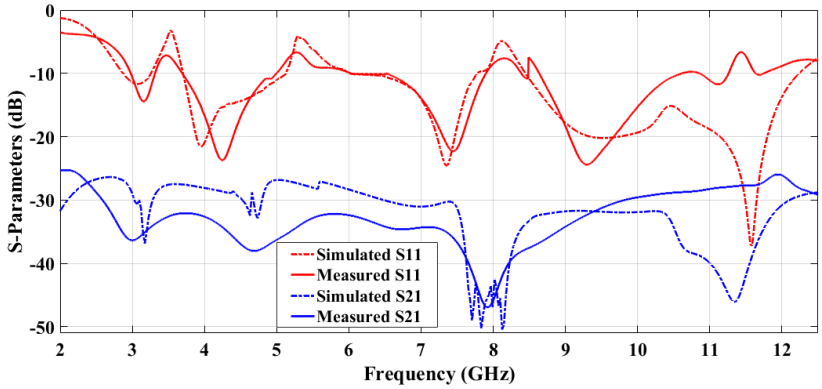

Figure 9. Simulated and measured S-parameters.

entire UWB range with frequency notching functions at 5.15–6 GHz, 7.8–8.4 GHz, and 3.3–3.7 GHz. So, the designed antenna can efficiently suppress the potential interference from WLAN, X-band satellite communication, and WiMax systems. It is also found from Fig. 9 that the simulated and measured S_{21} are higher than 25 dB from 3 to 11 GHz indicating good isolation between antenna ports. Good agreement between measured and simulated results is identified except some deviations probably due to dielectric and conductor losses, fabrication imperfections, soldering, SMA connector effects and measurement tolerances.

3.2. Radiation Patterns, Gain, and Efficiency

The measured and simulated radiation patterns of an antenna on the E-plane (XZ) and H-plane (YZ) at 3.1, 4.5, 7.3, and 9.5 GHz with port-1 excited and port-2 matched with 50-ohms, and vice versa are

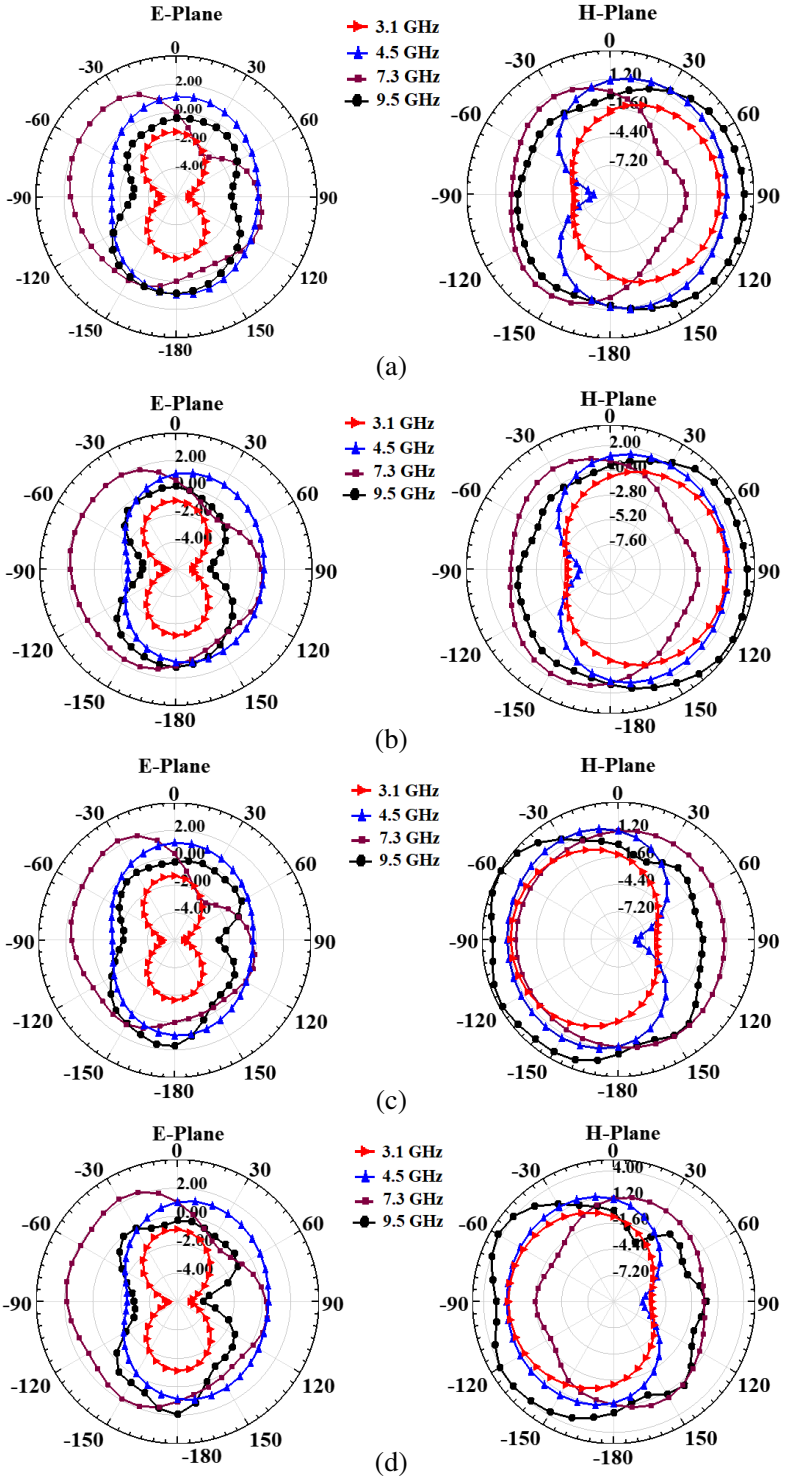

Figure 10. Radiation patterns at 3.1, 4.5, 7.3, and 9.5 GHz when (a) measured-port-1 excited, (b) simulated-port-1 excited, (c) measured-port-2 excited, and (d) simulated-port-2 excited.

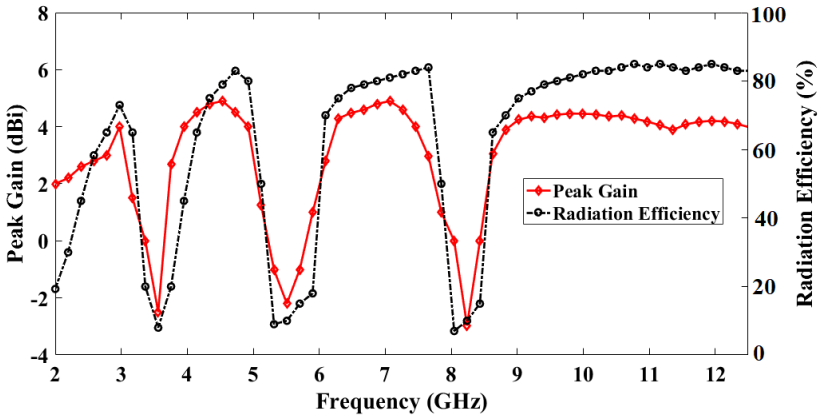

Figure 11. Measured peak gain and radiation efficiency.

plotted in Figs. 10(a)–10(d). Good agreement between measured and simulated radiation patterns is found from Fig. 10. It can also be observed that the proposed antenna has a dipole-shaped pattern in E-plane and quasi-omnidirectional pattern in H-plane. The quasi-omnidirectional pattern in H-plane is desired for portable UWB wireless communication systems to receive signals from all directions so that the orientation of system will have no effect. From Figs. 10(a) and 10(c), it can be seen that radiation patterns in the H-plane are mirror images. Hence, the proposed antenna offers pattern diversity. Fig. 11 displays the measured peak gain and radiation efficiency of the proposed antenna. It can be observed that the proposed antenna has peak gains from 2 to 5 dBi and radiation efficiency above 80% across the UWB band except at notched bands. At notched bands, the peak gains dramatically drop to around -2.5 dBi, and efficiencies are about 8% showing that the proposed antenna effectively mitigates the potential interference from narrowband systems.

3.3. Diversity Performance

In addition to radiation patterns, the envelope correlation coefficient (ECC) is another key parameter to describe the diversity performance of MIMO antenna. The measured and simulated ECC values are computed from S-parameters using Equation (6) of the two-port MIMO antenna proposed by Blanch et al. [29].

$$ECC = \frac{|S_{11}^{*}S_{12} + S_{21}^{*}S_{22}|^2}{(1-(|S_{11}|^2+|S_{21}|^2))(1-(|S_{22}|^2+|S_{12}|^2))}, \tag{6}$$

The measured and simulated ECC values of the proposed antenna with respect to frequency are

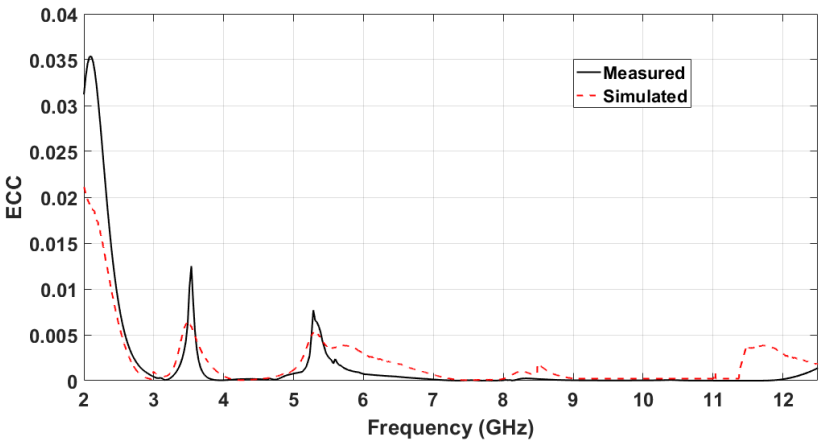

Figure 12. Measured and simulated envelope correlation coefficient of the proposed antenna.

displayed in Fig. 12. It is observed that small discrepancy between these two values is observed because of fabrication tolerances. The results show that all the ECC values are well below 0.013 over the entire UWB band demonstrating that the proposed antenna is a suitable candidate for UWB MIMO systems.

The performance comparison of the proposed antenna with existing UWB-MIMO antennas in the literature is given in Table 1. It can be observed that the proposed antenna performance in terms of antenna overall size, impedance bandwidth, mutual coupling, peak gain, and ECC is appreciable compared with the published designs which are listed in Table 1. In [23], a trident-shaped strip was loaded on the microstrip line to obtain dual notched bands at WLAN and X-bands. However, in the proposed design, triple band-notches at WLAN, X-band, and WiMax are achieved by placing two C-shaped slots on radiating patches and U-shaped strips added to ground.

Table 1. Performance comparison of various published designs with the proposed antenna.

Ref. No.	Antenna overall size (mm^3)	Bandwidth (GHz)	Mutual coupling, $\lvert S_{21}\rvert$ (dB)	Peak gain (dBi)	ECC	No. of notched-bands
[13]	$22 \times 36 \times 1.6 = 1267.2$	3.1–11	< -15	2–7	< 0.06	1
[14]	$43 \times 20 \times 0.762 = 655.32$	3.1–10.6	< -20	2.6–4.4	< 0.04	1
[16]	$22 \times 29 \times 0.8 = 510.4$	3–11	< -15	4.5–5.5	< 0.265	1
[19]	$27 \times 30 \times 0.8 = 648$	3–11	≤ -20	NA	< 0.012	2
[21]	$30 \times 30 \times 0.8 = 720$	3.5–10.6	< -15	NA	< 0.03	2
[22]	$35 \times 23 \times 1.6 = 1288$	3.1–10.9	< -17	NA	< 0.015	2
[23]	$22 \times 26 \times 0.8 = 457.6$	3.1–11.8	< -20	3.6-6.0	< 0.03	2
[24]	$30 \times 60 \times 1 = 1800$	2.8–11	< -20	1.5–5.0	< 0.035	3
[25]	$28 \times 22 \times 0.8 = 492.8$	3.1–10.6	< -18	0.6–4.5	< 0.02	3
[26]	$26.75 \times 41.5 \times 1.6 = 1776.2$	3.1–11.5	< -19	1.13–3.88	< 0.01	3
Pro. Ant.	$18 \times 21 \times 0.8 = 302.4$	2.8–12.2	< -25	2–5	< 0.013	3

4. CONCLUSION

To suppress the potential interference from existing narrowband systems, a compact UWB MIMO antenna with triple band-notched properties at WLAN, X-band satellite communication, and WiMax bands has been designed, fabricated, and tested. The measured results show that the proposed antenna can operate in the entire UWB band with an impedance bandwidth from 2.8 to 12.2 GHz. Low mutual coupling of $|S_{21}| < -25$ dB is achieved by adding a T-shaped stub to the ground plane. Triple band-notched functions are realized by placing two C-shaped slots on radiating monopoles and U-shaped strips extended from the ground. Moreover, the proposed antenna has better radiation properties and low ECC (< 0.013) across the UWB band compared to the designs mentioned in the literature. Performance comparison of various designs with the proposed antenna is also presented. Thus, the proposed MIMO antenna is a suitable candidate for portable UWB applications.

ACKNOWLEDGMENT

Authors would like to express their gratitude towards University College of Engineering & Technology, Acharya Nagarjuna University, Guntur and management of Koneru Lakshmaiah Education Foundation, Guntur for their continuous support and encouragement during this work. Further, J. Chandrasekhar Rao and Dr. N. Venkateswara Rao would like to acknowledge with thanks DST through FIST grant SR/FST/ETI-316/2012 and ECR/2016/000569.

REFERENCES

1. Federal Communications Commission (FCC), Revision of Part 15 of the Commission's Rules Regarding Ultra-Wideband Transmission Systems First Rep. and Order, ET Docket 98-153, FCC 02-48, Adopted: Feb. 2002; Released, Apr. 2002.
2. Kaiser, T., Z. Feng, and E. Dimitrov, "An overview of ultra-wide-band systems with MIMO," *Proceedings of the IEEE*, Vol. 97, 285–312, Feb. 2009.
3. Ben, I. M., L. Talbi, M. Nedil, and K. Hettak, "MIMO-UWB channel characterization within an underground mine gallery," *IEEE Trans. Antennas Propagation*, Vol. 60, No. 10, 4866–4874, 2012.
4. Zheng, L. and N. C. Tse, "Diversity and multiplexing: A fundamental trade-off in multiple-antenna channels," *IEEE Trans. Inf. Theory*, Vol. 49, No. 5, 1073–1096, 2003.
5. Zhang, S., Z. N. Ying, J. Xiong, and S. L. He, "Ultrawideband MIMO/diversity antennas with a tree-like structure to enhance wideband isolation," *IEEE Antennas and Wireless Propagation Letters*, Vol. 8, 1279–1282, 2009.
6. Liu, L., S. W. Cheung, and T. I. Yuk, "Compact MIMO antenna for portable devices in UWB applications," *IEEE Trans. Antennas Propagation*, Vol. 61, 4257–4264, 2013.
7. Zhang, S. and G. F. Pedersen, "Mutual coupling reduction for UWB MIMO antennas with a wideband neutralization line," *IEEE Antennas and Wireless Propagation Letters*, Vol. 15, 166–169, 2016.
8. Luo, C. M., J. S. Hong, and L. L. Zhong, "Isolation enhancement of very compact UWB-MIMO slot antenna with two defected ground structures," *IEEE Antennas and Wireless Propagation Letters*, Vol. 14, 1766–1769, 2015.
9. Li, H., J. Liu, Z. Wang, and Y.-Z. Yin, "Compact 1×2 and 2×2 MIMO antennas with enhanced isolation for ultrawideband application," *Progress In Electromagnetics Research C*, Vol. 71, 41–49, 2017.
10. Tao, J. and Q. Feng, "Compact ultrawideband MIMO antenna with half-slot structure," *IEEE Antennas and Wireless Propagation Letters*, Vol. 16, 792–795, 2017.
11. Zheng, Z. A., Q. X. Chu, and Z. H. Tu, "Compact band-rejected ultrawideband slot antennas inserting with $\lambda/2$ and $\lambda/4$ resonators," *IEEE Trans. Antennas Propagation*, Vol. 59, No. 2, 390–397, 2011.
12. Gao, P., S. He, X. Wei, Z. Xu, N. Wang, and Y. Zheng, "Compact printed UWB diversity slot antenna with 5.5-GHz band-notched characteristics," *IEEE Antennas and Wireless Propagation Letters*, Vol. 13, 376–379, 2014.
13. Liu, L., S. W. Cheung, and T. I. Yuk, "Compact MIMO antenna for portable UWB applications with band-notched characteristic," *IEEE Trans. Antennas Propagation*, Vol. 63, No. 5, 1917–1924, 2015.
14. Sipal, D., M. P. Abegaonkar, and S. K. Koul, "Compact band-notched UWB antenna for MIMO applications in portable wireless devices," *Microwave and Opt. Tech. Lett.*, Vol. 58, No. 6, 1390–1394, 2016.
15. Tao, J. and Q. Y. Feng, "Compact isolation-enhanced UWB MIMO antenna with band-notch character," *Journal of Electromagnetic Waves and Applications*, Vol. 30, No. 16, 2206–2214, 2016.
16. Liu, Z., X. Wu, Y. Zhang, P. Ye, Z. Ding, and C. Hu, "Very compact 5.5 GHz band-notched UWB-MIMO antennas with high isolation," *Progress In Electromagnetics Research C*, Vol. 76, 109–118, 2017.
17. Tripathi, S., A. Mohan, and S. Yadav, "A compact MIMO/diversity antenna with WLAN band-notch characteristics for portable UWB applications," *Progress In Electromagnetics Research C*, Vol. 77, 29–38, 2017.
18. Chu, Q. X. and Y. Y. Yang, "A compact ultrawideband antenna with 3.4/5.5 GHz dual band-notched characteristics," *IEEE Trans. Antennas Propagation*, Vol. 56, No. 12, 3637–3644, 2008.
19. Li, J. F., Q. X. Chu, and T. G. Huang, "Compact dual band-notched UWB MIMO antenna with high isolation," *IEEE Trans. Antennas Propagation*, Vol. 61, 4759–4766, 2013.

20. Tang, T. C. and K. H. Lin, "An ultrawideband MIMO antenna with dual band-notched function," *IEEE Antennas and Wireless Propagation Letters*, Vol. 13, 1076–1079, 2014.
21. Zhu, J., B. Feng, B. Peng, L. Deng, and S. Li, "Dual notched band MIMO slot antenna system with Y-shaped defected ground structure for UWB applications," *Microwave and Opt. Tech. Lett.*, Vol. 58, No. 3, 626–630, 2016.
22. Li, J.-F., D.-L. Wu, and Y.-J. Wu, "Dual band-notched UWB MIMO antenna with uniform rejection performance," *Progress In Electromagnetics Research M*, Vol. 54, 103–111, 2017.
23. Jetti, C. R. and V. R. Nandanavanam, "Trident-shape strip loaded dual band-notched UWB MIMO antenna for portable device applications", *Int. J. Electron. Commun.*, Vol. 83, 11–21, 2018.
24. Huang, H., Y. Liu, S. S. Zhang, and S. X. Gong, "Compact polarization diversity ultrawideband MIMO antenna with triple band-notched characteristics," *Microwave and Opt. Tech. Lett.*, Vol. 57, 946–953, 2015.
25. Yang, Z. X., H. C. Yang, J. S. Hong, and Y. Li, "A miniaturized triple band-notched MIMO antenna for UWB application," *Microwave and Opt. Tech. Lett.*, Vol. 58, No. 3, 642–647, 2016.
26. Banerjee, J., A. Karmakar, R. Ghatak, and D. R. Poddar, "Compact CPW-fed UWB MIMO antenna with a novel modified Minkowski fractal defected ground structure (DGS) for high isolation and triple band-notch characteristic," *Journal of Electromagnetic Waves and Applications*, Vol. 31, No. 15, 1550–1565, 2017.
27. Sharma, M., Y. K. Awasthi, and H. Singh, "Design of CPW-fed high rejection triple band-notch UWB antenna on silicon with diverse wireless applications," *Progress In Electromagnetics Research C*, Vol. 74, 19–30, 2017.
28. Sharma, M., Y. K. Awasthi, H. Singh, R. Kumar, and S. Kumari, "Compact UWB antenna with high rejection triple band-notch characteristics for wireless applications," *Wireless Pers. Commun.*, Vol. 97, No. 3, 4129–4143, 2017.
29. Blanch, S., J. Romen, and I. Corbella, "Exact representation of antenna system diversity performance from input parameter description," *Electronics Letters*, Vol. 39, 705–707, 2003.